


Review

# A Performance Evaluation of a Solar Air Heater Using Different Shaped Ribs Mounted on the Absorber Plate—A Review

Varun Kumar B. <sup>1</sup>, G. Manikandan <sup>1</sup>, P. Rajesh Kanna <sup>2,\*</sup> , Dawid Taler <sup>3</sup>, Jan Taler <sup>4</sup>, Marzena Nowak-Ocłoń <sup>4</sup>, Karol Mzyk <sup>4</sup> and Hoong Thiam Toh <sup>5</sup>

<sup>1</sup> Velammal College of Engineering and Technology, Madurai 625009, India; bvarunkumar09@gmail.com (V.K.B.); gmk@vcet.ac.in (G.M.)

<sup>2</sup> College of Engineering and Computing, Alghurair University, Dubai 37374, UAE

<sup>3</sup> Faculty of Environmental Engineering, Cracow University of Technology, 31-864 Cracow, Poland; dtaler@pk.edu.pl

<sup>4</sup> Faculty of Mechanical Engineering, Institute of Thermal Power Engineering, Cracow University of Technology, 31-864 Cracow, Poland; taler@mech.pk.edu.pl (J.T.); mnowak@mech.pk.edu.pl (M.N.-O.); karolm.1994@gmail.com (K.M.)

<sup>5</sup> Malaysia-Japan International Institute of Technology, Universiti Teknologi Malaysia International Campus, Jalan Semarak, Kuala Lumpur 54100, Malaysia; ht\_toh@yahoo.com

\* Correspondence: prkanna@gmail.com; Tel.: +971-5-0716-8906

Received: 14 September 2018; Accepted: 25 October 2018; Published: 9 November 2018



**Abstract:** In this paper, the effect of various shapes of ribs used in Solar Air Heaters (SAHs) was discussed. The review is concentrated on the geometry of the rib and its location on the SAH panel. Both numerical and experimental works were considered for discussion with dry air and Nano fluids as a working fluid. The influence of various shapes, such as an L shape, W shape, V shape, Multiple V shape, V shape with a gap, detachable & attachable ribs etc., was analyzed. The common fact observed from this analysis is that the implementation of artificial roughness in the absorber plate results in a considerable increase in the rate of heat transfer. Further, it is observed that ‘Multiple V-shaped with open between the ribs’ results in the maximum thermal enhancement when compared to the other shapes.

**Keywords:** shape of rib; solar air heater; heat transfer; friction factor

## 1. Introduction

Solar energy is abundantly available worldwide. Solar energy is an important alternative resource used in domestic and industrial applications like solar air heaters, solar lights, solar pumps, Photovoltaic applications, and many more, to meet the energy demand. Among these, the Solar Air Heater plays a major role in agriculture and rural areas for drying the crops, vegetables, heating the space etc. An SAH is simple to design and also economic. In the application of an SAH, it was found that using a smooth duct for the absorber plate led to a poor thermal efficiency by reason of less relative heat transfer. To increase the rate of thermal efficiency in a fluid, an artificial roughness is created closer to the surface, which results in recirculation of the fluid to create turbulence.

Implementing passive techniques in an absorber plate by using irregular forms like ribs, grooves, baffles, winglets, and twisted tapes, increases the heat transfer enhancement in solar duct [1–3]. Numerous authors [4–7] have conducted analytical and experimental investigations implementing passive techniques in absorber plates that resulted in heat transfer enhancement. The main goal of this review paper is to provide information about the importance of a rib molded on: (a) Different shaped

ribs, (b) the location of the rib by varying the Pitch distance, (c) height variation between two ribs, and (d) using multiple ribs mounted in inline and staggered methods. Based on various evaluators' studies, it is shown that the Discrete Multiple V shape with a staggered rib gives the best thermal performances when compared with other rib shapes and sizes. A detailed discussion is presented, based on the position and shape of a rib from the open literature.

## 2. Literature Survey

### 2.1. Various Shape of Ribs

#### 2.1.1. Numerical Investigation

Schematics of various geometries with the numerical investigation are listed in Table 1.

#### a. Grooves and Ribs Collective with Delta-Winglet Vortex (DWV)

Lei Luo, et al. [1] conducted a simulation investigation of various shapes, such as triangular grooves and perturbation triangular ribs, with additional shapes like semi-cylinder grooves and perturbation semi-cylinder ribs with delta-Winglet Vortex, including a consideration of Reynolds number range from 4000 to 40,000. Lei Luo, et al. [1] revealed that perturbation semi-cylinder ribs result in the best thermal enhancement due to strong rotation formation and the semi-cylinder grooves-shaped rib, together with DWVGs, show the maximum thermal enhancement.

#### b. Rectangular Sectioned Tapered Rib

L. Varshney, et al. [2] numerically examined 12 different types of tapered shape of rectangular rib considering taper angle of  $1.6^\circ$ ,  $2.3^\circ$ , and  $3.2^\circ$  for a pitch distance of 10, 15, 20, and 25 mm. The authors used the Renormalization Group method in the k- $\epsilon$  turbulence model with the selection of a wall enhanced function in the range of Reynolds number 3800 to 18,000. Their result reveals that the angle of  $1.6^\circ$  shows the maximum enhancement with index increases from 1.31 to 1.91. A Relative roughness pitch,  $P/e = 10.7$  with Re no ranges 12,000 displays the best performance in heat transfer.

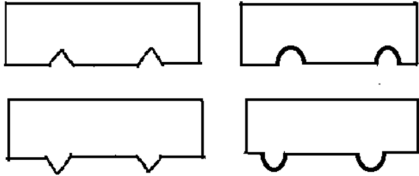
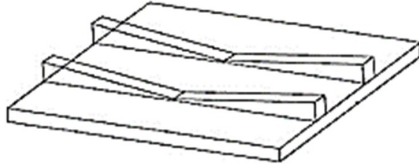
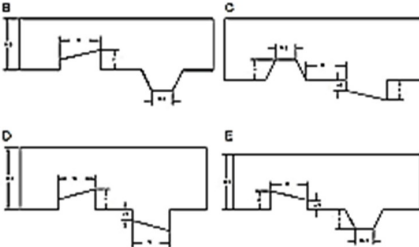
#### c. Rib–Groove Shapes (R-GR)

Ali Najah Al-Shamani, et al. [3] conducted simulation work for four different rib-groove shapes (Table 1, S. No 3) in a channel using nanoparticles with different volume fractions in the Reynolds number, which varied from 10,000 to 40,000. The report revealed that a new novel Trapezoidal groove shape shows the best heat transfer rate with a decent Nusselt number.

#### d. Sixteen Different Rib Shapes

Mi-Ae Moon, et al. [4] numerically examined 16 different shapes of rib with the pitch ratio of 10, the height of pitch 0.047, and a hydraulic diameter of 34 mm. The (SSG) Speziale-Sarkar-Gatski pressure–strain model was selected to analyze the turbulence. The Reynolds number was fixed in the range of 5000 to 50,000, with a rib pitch to width ratio of 5.0 to 10.0. The investigator declared that the result of the boot-shaped rib shows good heat transfer enhancement with less pressure drop than the square rib.

**Table 1.** Schematics of various geometries with the numerical investigation.

S. No	Shape	Parameter/Range	Remarks
1	Delta-Winglet Vortex Adapted from [1] 	Maximum heat transfer enhancement increased 51.6%.  Friction factor increases up to 6.11%.	Combination of DWV and semi-cylinder provide high heat transfer.
2	Rectangular Sectioned Tapered Rib Reproduced with Permission from [2], Elsevier, 2017 	12 different types of tapered rib with taper angle at 1.6°, 2.3° and 3.2° for the pitch of 10, 15, 20, and 25 mm are analyses.	1.91 corresponding to the angle of 1.6° shows maximum thermal enhancement.
3	Rib-Groove shapes Reproduced with Permission from [3], Elsevier, 2015 	Nanoparticles like Al <sub>2</sub> O <sub>3</sub> , CuO, SiO <sub>2</sub> , and ZnO <sub>2</sub> with volume fraction 1.4% taken.	Trapezoidal groove shape of rib shows the topmost heat transfer and best Nusselt number.

### 2.1.2. Experimental Investigation

Schematics of various geometries with the experimental investigation are shown in Table 2.

#### a. Broken Arc Rib (BAR)

Experimental and numerical simulations using the CFD technique were carried out by Gill R.S, et al. [5], and a broken arc-shaped rib collective with a staggered rib shape of a piece with the ratio of 12 was taken for analysis. Rib raggedness that was immovable with a staggered rib position of 0.4, roughness height of 0.043, gap size of 1.0, arc angle of 30°, and gap location of 0.65 with a roughness pitch of 10mm was considered. The staggered rib proportions were nominated from 1 to 6 with the Reynolds number ranging from 2000 to 16,000. The result shows that the comparison of the broken arc rib with a smooth channel revealed that the thermo-hydraulic performance of the duct attained the best performance and found that the highest value of the staggered rib size was 4.

#### b. Reverse L Shape Rib (RLSR)

Vipin B, et al. [6] numerically and experimentally investigated the reverse L shape rib with a relatively rough surface, with pitch varying from 7.14 to 17.86, the Re no ranging from 3800 to 18,000, and heat flux of 1000 W/m<sup>2</sup> taken for analysis, and the relative roughness height of e/D 0.042 was selected for the investigation. Here, the analytical results were related to observational results and found that the best achievement occurred for the range of parameters investigated. The authors revealed that thermal improvement in the Nusselt number was 2.9 times better than the normal duct.

### c. Arc Shape Ribs Set in 'S' Shape (SR)

Experimental research was conducted by Khushmeet Kumar, et al. [7] with circular wire arc shape ribs, which were placed in an 'S' shape formation in the duct within an arc angle varying from ( $\alpha$ ) of  $30^\circ$  to  $75^\circ$  with a relative roughness pitch ( $P/e$ ) 4 to 16mm and relative roughness width ( $W/w$ ) of 1 to 4mm in the range of Re no 2400 to 20,000. Implementing this "S"-shaped rib results in a higher augmentation in the friction factor ( $f$ ) and better Nusselt number ( $Nu$ ), and it was found that the best thermal enhancement was achieved at an arc angle ( $\alpha$ ) of  $60^\circ$ .

### d. W-Shaped Rib (WSR)

AtulLanjewar, et al. [8] experimentally investigated thermal performances and friction factor ( $f$ ) with novel 'W'-shaped ribs placed in a rectangular duct on its underneath on one side of the wall prepared at a  $60^\circ$  inclination admiration to the fluid flow direction. The study considered a duct hydraulic diameter ratio equal to 8.0, a relative roughness height ( $e/D_h$ ) fixed in the range from 0.018 to 0.03375, a relative roughness pitch ( $p/e$ ) of the rib equal to 10, and an attack angle from  $30^\circ$  to  $75^\circ$ . The Reynolds number used ranged from 2300 to 14,000. They declared that the 'W' shape of the rib at a  $60^\circ$  attack angle gave the best thermal performance and friction factor when related with the smooth duct.

### e. Different Shape-Rib (DV-R)

Giovanni Tanda [9] conducted an experimental investigation of various shapes of rib-like (a) transverse continuous ribs, (b) angled continuous ribs, and used other novel shapes of (c) broken ribs and (d) discrete V-shaped ribs. The author considered that repeated ribs in a duct promote an effective performance to enhance the friction factor and thermal coefficients. The study experimentally examined a rectangular channel with uniform heat flux at one wall roughened by repeated ribs and the remaining three walls were fixed as smooth and insulated. The result revealed that all the implementing ribs roughened in channels achieved better agreement than the smooth duct.

### f. Triangular-Rib with Triangular-Groove (TR)

Experimental research conducted by Smith Eiamsa-ard, et al. [10] using three types of rib-groove arrangement with the parameters of  $W/H$  equal to 20, height of the duct  $H$  equal to 9 mm, rib height set as  $e$  equal to 3 mm, and three different pitch ratios  $P/e$  of 6.6, 10, and 13.3. The results support the idea that using a Triangular-Rib with a Triangular-Groove-shaped rib shows that thermal enhancement obtained the highest values for all pitch ratios at a constant pumping power.

### g. Protruded Roughness Geometry (PR)

BrijBhushan and Ranjit Singh [11] conducted an experimental investigation for better enhancement of the Nusselt number and friction factor using a protruded smoothness novel geometry in the duct. They compared the result with a smooth duct. The investigation revealed that the maximum augmentation in the heat transfer coefficient was found for an ( $S/e$ ) way length of 31.25 and detailed values are shown in (Table 2, S. No 11).

### h. Transverse Ribs on One, Two, Three, and Four walls (TR)

P.R. Chandra, et al. [12] experimentally investigated a heat transfer rib in all four walls, one by one, with the Re no ranging from 10,000 to 80,000. The pitch in the direction of the rib height ratio  $P/e$  was set as 8 and height of the rib in the direction of the channel hydraulic diameter ratio  $e/D_h$  was 0.0625. The result shows that the heat transfer roughness,  $G(e)$ , augmented with roughness.



**Table 2.** Schematics of various geometries with experimental investigations.

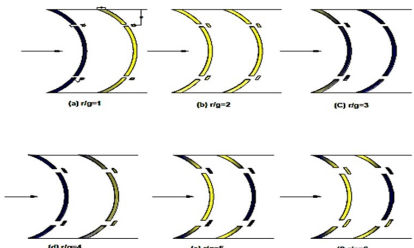
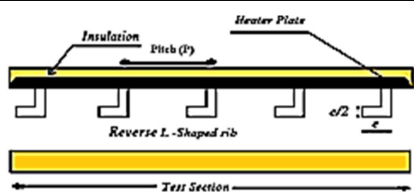
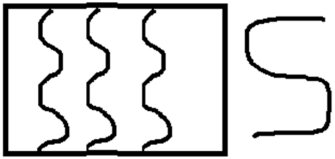
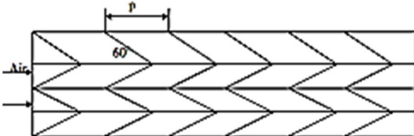
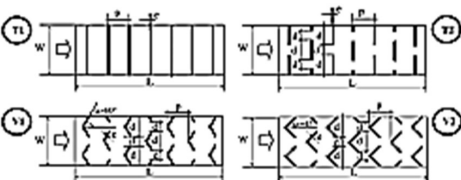
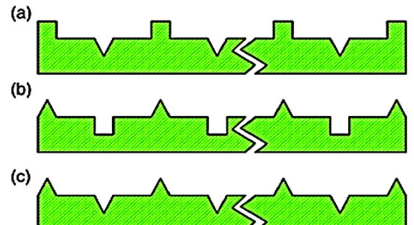
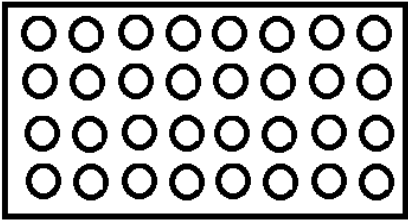
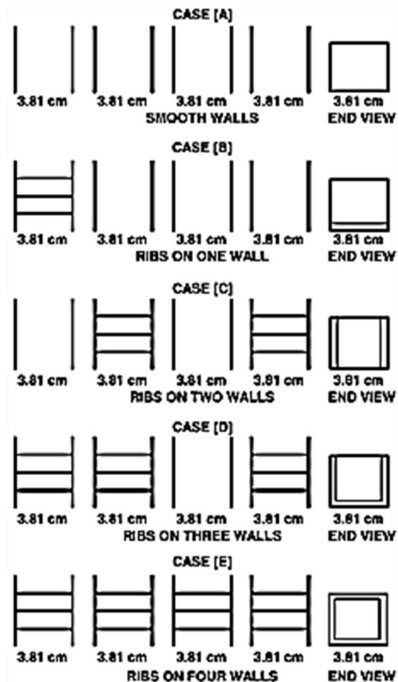
S. No	Shape	Parameter/Range	Remarks
Broken Arc Rib Adapted from [5]			
1		<p>Nusselt Number Result Shows in</p> <p>With staggered rib, 3.06 and 2.50.</p> <p>Without staggered rib, 2.60 and 2.27.</p>	A staggered piece of rib placed between broken ribs induced a strong friction factor and Nusselt number.
Reverse L shape rib Reproduced with Permission from [6], Elsevier, 2016''			
2		Thermo hydraulic performance occurs between 1.62–1.90.	Reverse l shape rib increases thermal performance.
Arc shape wire ribs arranged in 'S' shape adapted from [7]			
3		Heat transfer augmentation and friction factor relative to arc shape significance 0.6667.	A survey was taken in an arc shape so they used a circular wire arc S shape rib for investigation.
W-shaped rib Reproduced with Permission from [8], Elsevier, 2011			
4		<p>Nusselt number 2.36</p> <p>Friction factor 2.01.</p> <p>Attack angle of 60°</p>	Using 60° attack angle, enhancement of Nusselt and friction factor will be greater and related with the smooth duct.
Different shape of rib Reproduced with Permission from [9], Elsevier, 2011			
5		<p>Thermal enhancement 0.013–0.014 (i.e., 13–14 K of air temperature upswing over the 1.5 m collector length with Re number near 7000.</p>	Best relative performance to the non-artificial channel is attained by the novel shape of transverse broken ribs.
Triangular-Rib with Triangular-Groove Reproduced with Permission from [10], Elsevier, 2009			
6		The aspect ratio of $W/H = 20$ and duct height = 9 mm with height of rib $e = 3$ mm at three various pitch ratios, $P/e = 6.6, 10$ , and 13.3.	Triangular-rib with triangular-groove provides the best values for all pitch ratios.

Table 2. Cont.

S. No	Shape	Parameter/Range	Remarks
Protruded Roughness Geometry Adapted from [11]			
7		(S/e) Length = 31.25, (L/e) relative long way length = 31.25 and (d/D) relative diameter = 0.294.	Protruded absorber plate shows the best heat transfer coefficient compared with the smooth plate.
Transverse ribs on 1, 2, 3 and 4 walls are reported Reproduced with Permission from [12], Elsevier, 2003			214% increase of Case B related to Case A.
8		Investigated transfer rib in all four walls, one by one.	72% increase in Case C related to Case B.  35% increase of Case D related to Case C.  30% increase of Case E related to Case D.

## 2.2. Various Pitch Distances

### 2.2.1. Numerical Investigation

Schematics of various pitch distances with the numerical investigation are shown in Table 3.

#### a. Hyperbolic Rib (HR)

Deep Singh Thakur, et al. [13] carried out a simulation analysis using FLUENT 15.0 for the hyperbolic rib with various parameters, including a pitch distance of 10–20 mm, a roughness height of the rib ranging from e 0.5 mm to 2 mm, and a Reynolds number of 10,000. By comparing the above parameters of HR with various shaped ribs, such as triangular, rectangular, and another novel shape like semicircular rib geometries, it was shown that the optimum performance of the hyperbolic rib is attained when e is equal to 1 mm and P is equal to 10 mm at the Re no of 6000. In this case, the Hyperbolic shape of a rib avoids the frame of small eddies in the corners at upstream and downstream sides where the friction factor is not high at rib height from 0.5 mm to 1.5 mm and the heat transfer is enhanced at a Reynolds number of 6000.

### b. Transverse Square Rib (TSR)

Anil Singh Yadav and Bhagoria J.L. [14] simulated a CFD code for a repeated transverse square sectioned rib. The authors examined 12 dissimilar position of a square sectioned rib with the following parameters: relative roughness height ranging from  $(e/D)$  0.021 to 0.042, relative roughness pitch  $(P/e)$  ranging from 7.14 to 35.71, and Re no ranging from 3800 to 18,000. They concluded that Re 12,000 produced a good thermo-hydraulic performance (THPP) equal to 1.88 and the best rib roughness shows an  $(e/D)$  value of 0.042 and  $(P/e)$  equivalent to 10.71.

### c. Discrete Multi V-Rib Through Staggered Rib

Anil Kumar and Man-Hoe Kim. [15] examined the influence of the roughness width ratio by the CFD technique by using the RNG-k- $\epsilon$  model and they analyzed the typical friction factor, Nusselt number, and overall thermal performance. The result of this case shows that the discrete multi V-rib using a staggered rib shape is 6% advanced when associated with further rib shapes. Anil Kumar and Man-Hoe Kim [15] found that the highest significance of the relative width ratio was 6.0.

### d. Square Ducts with Internal Surfaces Ribbed

Simulation work carried out by Kamali R. and Binesh A.R. [16] for various profiles of the rib included triangular and square, a newly arranged method of trapezoidal with diminishing height in the flow direction, and another arrangement of trapezoidal with augmentative height in the flow direction. The results reveal that the presence of rib scattering of the heat transfer coefficient is sturdily pretentious by the incidences of the rib profile and it shows that the best heat transfer augmentation occurred in the trapezoidal rib with diminishing height in the downstream flow direction.

### e. Broken V-Ribs (BV-R)

A numerical investigation was carried out by Promthaisong Pitak, et al. [17] in the 3D horizontal square channel with a broken V-rib, which was compared with and without a V-rib in the duct using open corner  $d/H$  values of 0, 0.01, 0.02, 0.03, 0.04, and 0.05. Promthaisong Pitak reported that using a broken V-Rib results in higher heat transfer and friction loss.

### f. Textured Asymmetric Arc Rib (TAR)

H.T. Wang, et al. [18] carried out a simulation in a single phase channel with a 2D interior surface with the Re no ranging from 20,000 to 60,000. The optimized symmetric triangular rib was taken for comparison with smooth flow and found that certain developments are closely correlated to the rise in fluid flow and improve the performance of thermal efficiency.

**Table 3.** Schematics of various pitch distances by the numerical investigation.

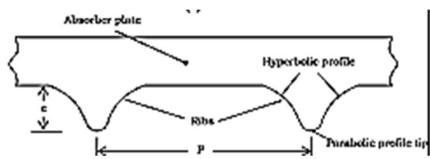
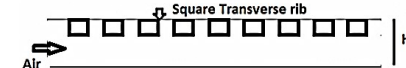
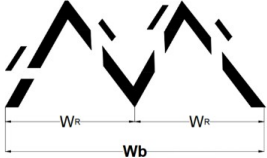
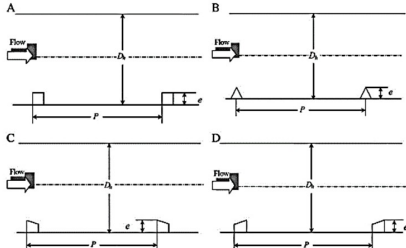
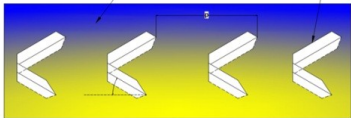
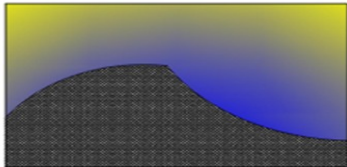
S. No	Shape	Parameter/Range	Remarks
1	Hyperbolic Rib Reproduced with Permission from [13], Elsevier, 2017 	Thermal-hydraulic performance.  Friction factor	Hyperbolic rib avoids entrapment of small eddies in the corners, heat transfer enhancement will increase, and a decrease of rib height causes reduction of friction factor.
2	Transverse square rib adapted from [14] 	Thermal-hydraulic performance factor varies between 1.22 and 1.88.	Presence of an Inner square section of the rib will produce better thermal performance.

Table 3. Cont.

S. No	Shape	Parameter/Range	Remarks
3	Discrete Multi V-Rib with Staggered Rib Adapted from [15] 	The overall thermal performance will be 3.67 with a width ratio of 3.0.	Staggered induct high velocity with turbulence in Discrete multiple v rib increases heat transfer coefficient.
4	Square Ducts with Internal Surfaces Ribbed Reproduced with Permission from [16], Elsevier, 2008 	The P/e ratio of 12 provides the highest augmentation.	Inter rib distribution heat transfer strongly affects the shape of rib and recirculation just behind rib will be sensitive.
5	Broken V-ribs Adapted from [17] 	Broken V-rib compared without V-rib in following parameter: $d/H = 0, 0.01, 0.02, 0.03, 0.04, \text{ and } 0.05$ .	Broken-V Rib leading higher heat transfer enhancement about 346–539%.
6	Textured Asymmetric Arc Rib Adapted from [18] 	$p/e = 5$ for the compound rib with $d/e = 0.06$ and $p/e = 6$ for triangular rib and asymmetric arc rib.	Progressive compound rib could progress the recital of heat transfer.

## 2.2.2. Experimental Investigation

Schematics of various pitch distances with the experimental investigation are shown in Table 4.

### a. Integral Chamfered Rib (ICR)

Rajendra Karwa, et al. [19] experimentally investigated ICR with relative roughness pitch from 4.58 to 7.09 and the rib chamfer angle fixed at  $15^\circ$ . Airflow in a duct with depth values of 21.8 mm, 21.5 mm, and 16 mm was tested with relative roughness heights for the three roughness plates values of 0.0197, 0.0256, and 0.0441, respectively. The Reynolds number varied from 3750 to 16,350. The investigational study shows that the use of an integral chamfered rib significantly enriched the thermal efficiency from 10% to 40% in SAH.

### b. Effect of a Gap in the Inclined Rib

An experimental investigation work by Aharwal K.R., et al. [20] on the rectangular duct with a ratio of 5.83 investigated the effect of an opening in the inclined shape of a rib. The authors declared that the inclined rib allowing for a gap (inclined discrete rib) shows that enhanced heat transfer is related to a continuous inclined rib arrangement. The result shows that a 1.0 relative gap width in an inclined discrete rib produced good heat transfer when related to the further relative opening width.

### c. Combined Wavy-Rib and Groove Turbulators

SompolSkullong, et al. [21] carried out an experimental work on Combined Wavy-Rib and Groove turbulators with the Reynolds number ranging from 4000 to 21,000. To bring forth recirculation flow in the duct, triangular wavy ribs were used to repeatedly place it in a duct with heat-flux realistic on the upper wall. Three tests were carried out with dissimilar rib pitch to duct height ratios and the PR set as 0.5; in addition,  $P/H$  was set as 2. A single rib was placed in the channel height ratio of  $b/H$  equal to 0.25 with three different types of rib preparations, namely (a) rib—groove combination placed on upper wall only, (b) inline methods rib—groove arrangement, and (c) combination of staggered and inline rib groove on opposite sides of the walls. The wavy ribs were situated at a  $45^\circ$  attack angle inflow direction of the fluid. The authors declared that the highest thermal efficiency occurred at the upper wall of the ribbed-grooved specimen at PR equal to 0.5 and the combined rib-groove turbulator exhibited the over achievement of heat energy compared to the groove alone.

### d. Staggered-Winglet Perforated Tapes (S-WTR)

Sompol Skullong, et al. [22] experimentally investigated the staggered-winglet perforated tapes with the Reynolds Number ranging from 4180 to 26,000. Winglet perforated tapes had a winglet inclination angle of  $30^\circ$  with winglet blockage ratios  $B$  from 0.1 to 0.3. The highest thermal enhancement factor TEF equal to 1.71 was attained by applying the WPT with  $B$  RR equal to 0.15,  $P$  equal to 1.0,  $Re$  equal to 4180. The result reveals that the staggered-winglet perforated tapes with winglet perforated tapes yield a thermal enhancement factor that is about 1.2 times higher than the winglet non-perforated tape.

### e. Pairs of Trapezoidal-Winglets Groove and TW (T-WGR)

Sompol Skullong, et al. [23] discerned an experimental investigation with a pair of trapezoidal winglets and groove shape of the rib, with the  $Re$  no ranging from 4500 to 22,000 and the single angle of attack of  $45^\circ$ . Experimental outcomes show that the Trapezoidal-Winglets together with the Groove produce the maximum heat transfer and pressure drop increase in heat transfer over the smooth channel.

### f. Continuous Rib Turbulator (CR)

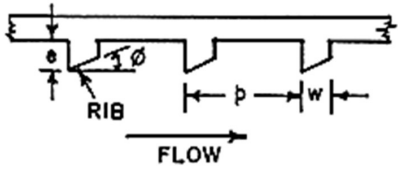
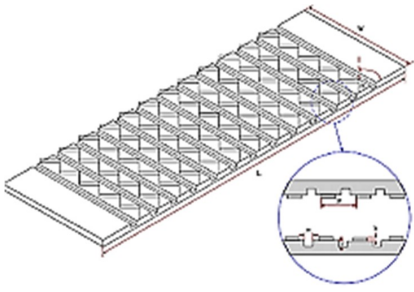
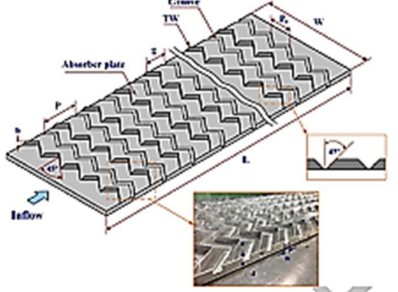
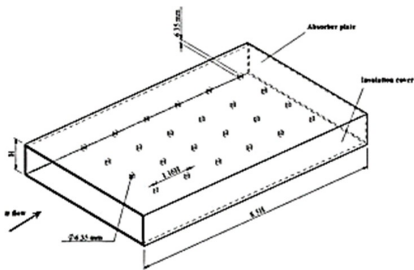
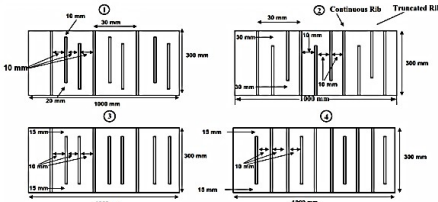
Mohammed O.A. et al [24] carried out an experimental investigation using solid inclined, curved and vertical baffles for swirls flow underside of the absorber plate. Investigators declared that the ribs in the cavity area that gradual increase of the Nusselt number and also a solid curved baffles placed in absorber plate shows best performance.

### g. Thin Ribs (TR)

Experimental and numerical research work was done by Sanjay K. Sharma, et al. [25] on the width to height  $W/H$  of 10 for the duct consuming obstacle ratio  $e/H$  of 0.1, with additional parameters like roughness height  $e/D$  of 0.055, roughness pitch  $P/e$  of 10, attack angle of  $90^\circ$ , and Reynolds number from 4000 to 16,000. The investigators claimed three important outcomes:

- (A) Rib arrangement 1 elucidated that midribs positioned at 3.3% and 6.67% truncation from the side walls provide the maximum thermal enhancement.
- (B) Arrangement 3 elucidated that middle ribs permanent at 5% truncation from side walls provide the better performances in terms of THPP results.
- (C) Arrangement 4 elucidated that with two transverse continuous ribs in between the truncated ribs, there was an indication of the maximum pressure drop.

**Table 4.** Schematics of various pitch distances with the experimental investigation.

S. No	Shape	Parameter/Range	Remarks
1	<p>Integral chamfered rib Reproduced with Permission from [19], Elsevier, 2001</p> 	<p>Nusselt number enhancement was 120% more than the smooth absorber plate.</p> <p>Friction factor 1.8 to 3.9.</p>	<p>Integral chamber rib will increase 7% thermal efficiency.</p>
2	<p>Combined Wavy-Rib and Groove turbulator Reproduced with Permission from [21], Elsevier, 2014</p> 	<p>Thermal Performance of about 49–52% achieved.</p>	<p>Rib pitch to channel height can apply groove alone to attain maximum thermal performance.</p>
3	<p>Trapezoidal-Winglets Groove Reproduced with Permission from [23], Elsevier, 2017</p> 	<p>Single attack angle of 45° considered.</p>	<p>Maximum heat energy transfer and pressure drop increased over the non-artificial channel.</p>
4	<p>Continuous Rib Turbulator Reproduced with Permission from [24], Elsevier, 2015</p> 	<p>Solid inclined, curved, and vertical baffles used for optimal flow.</p>	<p>Solid curved baffles placed nearby absorber plate show the best performance valuation.</p>
5	<p>Thin Ribs Reproduced with Permission from [25], Elsevier, 2017</p> 	<p>Aspect ratio for the duct (W/H) = 10, blockage ratio (e/H) = 0.1, roughness height (e/D) = 0.055, roughness pitch (P/e) = 10, and attack angle (a) = 90° are considered.</p>	<ol style="list-style-type: none"> <li>1. The highest Nusselt number augmentation is 49.28 in case 1.</li> <li>2. Highest augmentation regulated in friction factor is 2.88–7.18 in case 4.</li> </ol>



### 2.3. Various Angle of Rib

#### 2.3.1. Numerical Investigation

Schematics of the various angles of ribs with the numerical investigation are shown in Table 5.

##### a. 45° Inclined V Shape Rib (IVSR)

Ahmed M., et al. [26] conducted numerical simulations for a duct using six different rib configurations. Inline and staggered arrangement of the ribs is fixed in the top and bottom walls of the channel with an angle of 45° inclined and 45° V shape. All these shapes of ribs are associated with the 90° transverse ribs. Ahmed M. et al. [26] declared that 45° V-shaped ribs enhance the performance, inducing a strong rotation and increasing the heat transfer in the cross-sectional passage compared with 90° transverse ribs.

##### b. Discrete V-Down Rib (DV-DR)

Numerical investigations were carried out by Sukhmeet Singh, et al. [27] with a discrete V-down artificial raggedness rib compared with flat plate SAH to increase the pumping power flow rate. The limitations used were relative roughness pitch, position, width, height, and the angle of attack, which have a combined effect on heat transfer and fluid friction. The report shows that roughness parameters of the discrete V-down shape of rib for an assumed Reynolds number show the highest energetic efficiency.

##### c. Slit Rib (SR)

PankajParihar, et al. [28] numerically investigated heat transfer enhancement and pressure drop characteristics in a rectangular duct using slit ribs. The hydraulic diameter of the duct to rib height ratio was fixed as 0.094, whereas the rib pitch varied from 6 to just before 12 and the Reynolds number ranged from 10,000 to 50,000. Results attained the highest Nusselt number at an angle of  $\alpha = 65^\circ$  when the Reynolds number was equal to 50,000 at a pitch ratio  $p/e$  of 12, and the lowest friction factor was obtained at the irregularity angle of  $85^\circ$  with  $Re$  equal to 50,000.

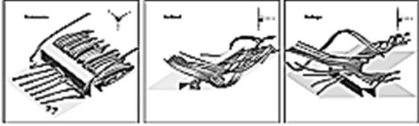
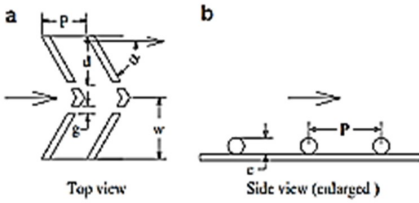
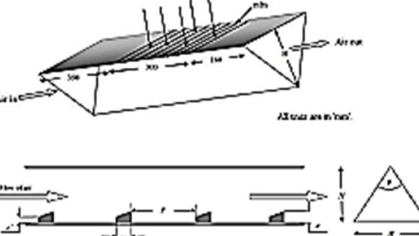
##### d. Nine Different Rib Shapes Compared with Two Turbulent Models

Simulation work was done by Alok Chaube, et al. [29] with nine different shapes of rib with Shear Stress Transport (SST), and the  $k-\omega$  turbulence model used in the analysis also compared heat transfer enrichment and the friction factor in the range of  $Re$  3000 to 20,000. They reveal that a rectangular rib size of  $5 \times 3$  mm resulted in the best heat transfer coefficient befalls at reattachment of the separated flow.

##### e. Forward Chamfered Ribbed (FCR)

Rajnesh Kumar, et al. [30] numerically studied a forward chamfered ribbed parameter of  $(e/w)$  0.24 to 1.5 with relative roughness height varying from  $(e/D)$  0.018 to 0.043 and  $e'/e$  ranging from 0 to 1.0. They declared that their result showed that the maximum Nusselt number increase occurred in the case of  $(e/w)$  1.5,  $(e/D)$  0.043, and  $(e'/e)$  value 0.75.

**Table 5.** Schematics of the various angles of ribs with the numerical investigation.

S. No	Shape	Parameter/Range	Remarks
1	<p>45° inclined V shape rib adapted from Journal of Applied Mathematics and Physics [26] scientific research</p> 	Heat transfer enhancement will be 230–580% higher than the smooth channel.	Ribs arranged in opposite wall which create strong rotational momentum to increase heat transfer.
2	<p>Discrete V-Down Rib Reproduced with Permission from [27], Elsevier, 2012</p> 	Exegetic efficiency for $DT/I > 0.0175 \text{ K m/W}$ .	Exergy discrete V-Down rib suggests increasing the efficiency of pumping power to solar air heater.
3	<p>9 Different Rib Shape [29]</p> <p>(a) Rectangular rib—<math>2 \times 3 \text{ mm}</math>, <math>4 \times 3 \text{ mm}</math>, and <math>5 \times 3 \text{ mm}</math> (w!e)</p> <p>(b) Square rib—<math>3 \times 3 \text{ mm}</math> (w!e)</p> <p>(c) Chamfered rib—Chamfer angle <math>F = 11, 13</math>, and <math>158</math></p> <p>(d) Semicircular rib—radius <math>r = 3 \text{ mm}</math></p> <p>(e) Circular rib—diameter <math>d = 3 \text{ mm}</math>.</p>	SST turbulence model used to compare the different shapes for turbulence models.	Turbulence intensity is initiate maximum at peak of the local heat transfer. Heat transfer is initiate at the reattachment points.
4	<p>Forward Chamfered Ribbed Reproduced with Permission from [30], Elsevier, 2017</p> 	The $e/w$ , relative 10 roughness height ( $e/D$ ), and $e'/e$ ranges from 0.24 to 1.5, 0.018 to 0.043, and 0 to 1.0, respectively.	Different values of $e/D$ , the Nu enhances, and friction factor is maximum in case of $e/D$ value of 0.043.

### 2.3.2. Experimental Investigation

Schematics of the various angles of ribs with the numerical investigation are shown in Table 6.

#### a. Arc-Shaped Wire Rib (ASR)

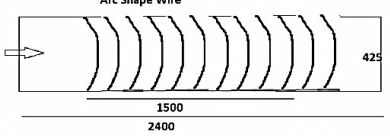
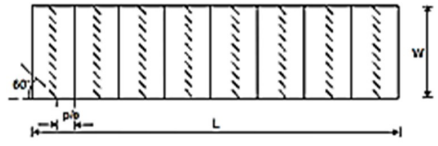
Saini S.K. and Saini R.P. [31] conducted an experimental investigation for enhancing turbulences by using an arc-shaped wire roughness element with relative roughness height ( $e/D$ ) and arc angle ( $a/90$ ), and the ( $Re$ ) varied from 2000 to 17,000. The author reveals moral agreement achieved between experimental measures and predicted values of Nu no and friction factor declared in SAH.

#### b. Combination of Inclined and Transverse Ribs (CI&TR)

Varun, et al. [32,33] experimentally looked into a combination of inclined and transfer ribs in a duct with the  $Re$  no ( $Re$ ) ranging from 2000 to 14,000, relative roughness pitch varying from ( $p/e$ ) 3 to 8, and relative roughness height set as ( $e=D$ ) 0.030. The result declared that the relative roughness pitch of 8 has the highest thermal efficiency. Varun et al. [33] investigated the same parameter using

the Taguchi method to optimize the thermal efficiency and revealed that this method can be effectively used for envisaging the solar air heater performance.

**Table 6.** Schematics of the various angles of ribs with the numerical investigation.

S. No	Shape	Parameter/Range	Remarks
1	<p>Arc-Shaped Wire Adapted from [31]</p> 	<p>The maximum improvement in Nusselt number has been obtained 3.80 times for the relative arc angle (<math>a/90</math>) of 0.3333 at relative roughness height of 0.0422.</p>	<p>Friction factor of 1.75 times of used parameters.</p>
2	<p>Combination of Inclined and Transverse Ribs Reproduced with Permission from [33], Elsevier, 2009</p> 	<p>Relative roughness pitch (<math>p/e</math>) 3–8 and relative roughness height (<math>e = D</math>) 0.030.</p>	<ol style="list-style-type: none"> <li>1. Relative roughness pitch of 8 has the highest thermal efficiency.</li> <li>2. Taguchi method used for optimal thermal efficiency.</li> </ol>

## 2.4. Multiple Ribs

### 2.4.1. Numerical Investigation

Schematics of multiple ribs with the numerical investigation are shown in Table 7.

#### a. Multi V Shape Rib (MVSR)

Anil Kumar [34] and Dongxu Jin et al. [35] both conducted CFD analysis of the Nusselt number and friction factor. Anil Kumar [34] used a different shape of artificial smoothness in the impressive of the thin circular wire in various shapes, namely (a) V-shaped, then arranged in (b) Multi V-shaped, and introduced another novel (c) Multi V-shaped rib with gap geometries for diverse turbulent models to investigate the heat transfer and pressure drop. The author choose Renormalization k-epsilon models for their analysis. Maximum heat transfer and pressure drop occurred in the novel Multi V-shaped ribs with a gap, which were compared with further shapes like V-shaped ribs and achieved good agreement. Dongxu Jin et al. [35] examined that effect of the span wise V-rib number in connection with a variable parameter such as attack angle, relative pitch, and relative height. They concluded that the maximum thermal performance was achieved at an attack angle of  $60^\circ$ , which provides the maximum value of the friction factor, and the authors revealed that using multi V-shaped ribs in a duct causes more stream wise helical vortex flow.

#### b. Non-Uniform Cross-Section in the Form of Saw-Tooth

A three-dimensional CFD investigation was carried out by Sukhmeet Singh, et al. [36]. They conducted a numerical experiment with the Re number ranging from 3000 to 15,000 in the transverse rib with non-uniform ribs like a square, trapezoidal, and circular rib. The k- $\epsilon$  turbulence model solution method was taken for the simulation investigation. They found that the maximum Nusselt number values occurred for the trapezoidal rib and a low friction factor occurred for the saw teeth rib.

#### c. Circular Transverse Wire Rib (CTWR)

Anil Singh Yadav and Bhagoria J.L. [37] extended their work in the numerical investigation for another shape of circular transverse wire rib by varying the Re no with relative roughness pitch ( $P/e$ ) and relative roughness height ( $e/D$ ) by using Renormalization-group (RNG) in the k- $\epsilon$  model. They showed that average Nusselt number and average friction factor values escalated with rib

height; however, this value decreased with pitch distance. The maximum thermal enhancement factor established was 1.65 greater than the smooth duct.

#### d. Conical Protrusion (CPR)

TabishAlam, et al. [38] conducted a numerical study using a conical protrusion rib and investigated the effect of relative ribs pitch  $p/e$  6 to 12 and relative ribs height  $e/D$  0.020 to 0.044 in the range of  $Re$  4000 to 16,000. The result found that a maximum thermal efficiency of 69.8% was achieved and the efficiency enhancement factor (EEF) was 1.346.

#### e. Discrete Double—Inclined Rib (DDR)

Ying Shuang Wang, et al. [39] completed an analytical work on the rectangular micro channel with a Discrete Double—Inclined rib. This double-inclined rib shape enhances heat transfer with the increasing height of the rib and number of double-inclined ribs, but the fluid flow resistance also increases at a similar time.

#### f. Downstream Ribs Arrangement

An analytical study was conducted by GongnanXie, et al. [40] in downstream ribs with six big continuous ribs mounted on one side of the wall with a pitch distances ratio of  $P/e$  equal to 20. It was initially designed in (Case A). Four cases were further designed, introducing half-size and same-size ribs downstream of the big ribs (Case B-E, respectively), shown in (Table 7, S. No 6). They declared that the downstream ribs are the best for decreasing the pressure loss and progressing the flow structure.

**Table 7.** Schematics of multiple ribs with the numerical investigation are presented.

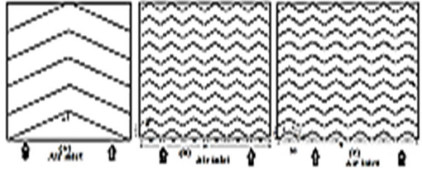
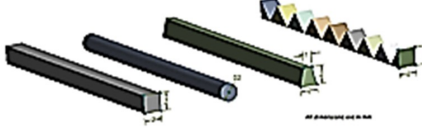
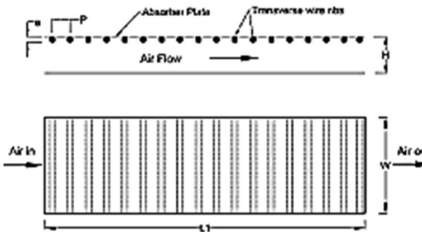
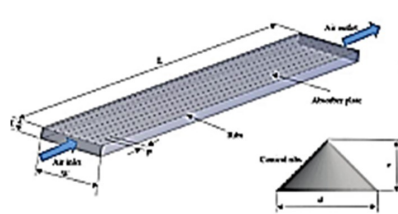
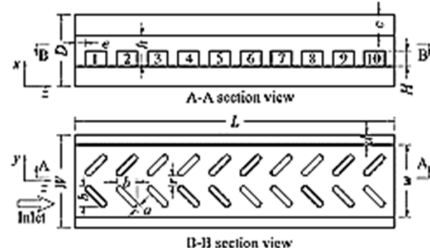
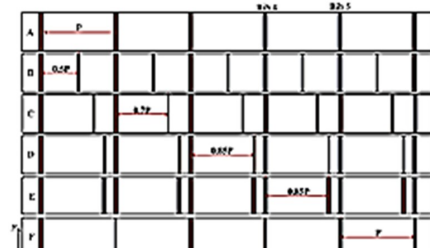
S. No	Shape	Parameter/Range	Remarks
1	Multi V shape rib Reproduced with Permission from [34], Elsevier, 2014 	Heat transfer enhancement increases from 1.7–5.6 compared with the smooth duct.	Multiple V shape rib compares smooth duct higher heat transfer taking place.
2	Non-Uniform Cross-section Ribs Reproduced with Permission from [36], Elsevier, 2015 	The trapezoidal rib has good Nusselt number range from 1.28 to 1.50. The square rib has a friction factor range from 2.64 to 3.74.	Compared with the square, circular, trapezoidal, and non-uniform, the trapezoidal shape has a good Nusselt number.
3	Circular Transverse Wire Rib Reproduced with Permission from [37], Elsevier, 2013 	Maximum average Nusselt number originates in 117 with relative pitch of 7.14 and relative height of 0.042.  Average friction factor originates in 0.00317 for relative height of 0.042 and relative pitch of 7.14.	Circular transverse wire rib with parameter of $P/e = 10.71$ and $e/D = 0.042$ affords better thermal enhancement.

Table 7. Cont.

S. No	Shape	Parameter/Range	Remarks
Conical Protrusion Reproduced with Permission from [38], Elsevier, 2017			
4		Nusselt number of 1.3 and friction factor of 1.0 are observed in conical protrusion ribs compared to the spherical ribs.	Maximum thermal efficiency is 69.8% and efficiency enhancement factor (EEF) is 1.346.
Discrete Double—Inclined Rib Reproduced with Permission from [39], Elsevier, 2014			
5		The height of the ribs and effects of the Re no are examined in mini-channel.	Enhance heat transfer with the increasing height and number of the double-inclined ribs.
Downstream Ribs Arrangement Reproduced with Permission from [40], Elsevier, 2013			
6		Different cases designed by introducing half-size and same-size ribs downstream of the big ribs.	It found downstream ribs decrease the pressure loss and increase the flow structure.

## 2.4.2. Experimental Investigation

Schematics of multiple ribs with the experimental investigation are shown in Table 8.

### a. Flow-Attack-Angle in V-Down Rib (AV-D R)

Sukhmeet Singh, et al. [41] conducted experimental work for five rib roughened plates with a flow-attack-angle ( $\alpha$ ) of  $30^\circ$  to  $75^\circ$ . The authors tested a duct with the aspect ratio AR of 12, with the relative roughness height set as 0.043 and relative roughness pitch as 8, with ranges of Re no from 3000 to 15,000. The thermo-hydraulic performance parameter power ( $g$ ), friction factor ( $f$ ), and Nusselt number ( $Nu$ ) were considered for analysis. The report found that the highest values show an angle of  $60^\circ$  and are related with the continuous V-down rib for the same rib-roughness parameters.

### b. Discrete Multi V-shaped and Staggered Ribs

Ravi Kant Ravi and Saini R.P. [42] experimentally analyzed the discrete multi V-shaped and staggered ribs with the Re no ranging from 2000 to 20,000 and the relative staggered rib size ranging from 1 to 2.5. It was shown that implementing the rib on every side of the plate in double pass mode results in higher heat transfer.

### c. Circular and V-Type Turbulators (V-Type)

Rajaseenivasan T. et al. [43] compared circular turbulators with V-type turbulators in inline and staggered methods for both experimental and theoretical work, and the ambient temperature reached an upper value of 66 °C in type-f, shown in (Table 8), with the flow velocity of 57.7 kg/h. The Nu no accelerated with the Re no and reached the maximum of 210 for type-f turbulators at a Re no of 11,615. The report stated that using a Zigzag arrangement of a circular type of turbulator produces the best thermal enhancement factor.

#### d. Criss-Cross Pattern Formed by 45° Angled Rib

Prashant Singh, et al. [44] experimentally and numerically conducted a study using an inline and staggered Criss-Cross inclined rib with the Re no ranging from 30,000 to 60,000. The result declared by the author showed that best Nusselt number in a duct was achieved in the ranges of 2.7 and 3.1 for inline and staggered methods of the rib and that the best thermal hydraulic performance achieved between 1.2 and 1.5.

#### e. Multiple-Arc Shaped with Gaps (ARCR)

N.K. Pandey, et al. [45] experimentally examined the Multiple-arc shaped with a gap using an Re no ranging from 2100 to 21,000 with an (e/D) roughness height ranging from 0.016 to 0.044 (four values), roughness pitch (p/e) choices of 4 to 16 steps of four values, an Arc angle ( $\infty$ ) set from 30° to 75° steps of four values, a roughness width (W/w) from 1 to 7 steps of five values, a relative gap distance (d/x) of 0.25–0.85 steps of four values, and a relative gap width (g/e) from 0.5 to 2.0 steps of four values. The results show that the extreme augmentation in Nu no of 5.85 times and friction factor of 4.96 times was achieved in the evaluation compared to the smooth duct.

**Table 8.** Schematics of multiple ribs with the experimental investigation.

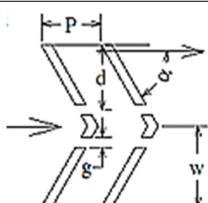
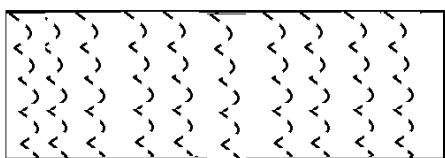
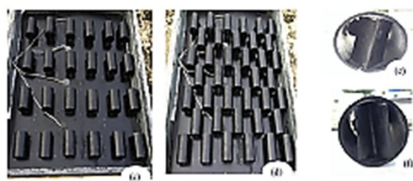
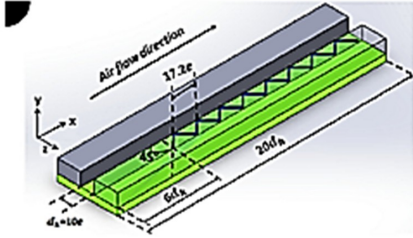
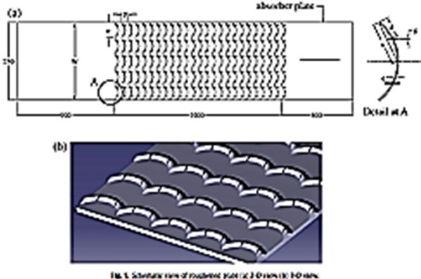
S. No	Shape	Parameter/Range	Remarks
1	Flow-attack-angle in V-Down rib Arrangement Reproduced with Permission from [41], Elsevier, 2012 	Highest thermo-hydraulic performance is 2.06 resultant to flow-attack-angle of 60°	A Nusselt number is a strong function in flow attack angle and varies from 30° to 70° attack angle
2	Discrete multi V shaped and staggered ribs Adapted from [18] 	Nusselt number ratio 3.4 Friction factor ratio 2.5.	Double pass channel with multiple v shapes will increase heat transfer rate compared with single pass channel.
3	Circular and V-Type Turbulators Reproduced with Permission from [43], Elsevier, 2015 	Thermal Enhancement factor is 3.65 at Re of 6200.	The zigzag prearrangement of circular tabulators with concave shape inserts exhibits best performance.



Table 8. Cont.

S. No	Shape	Parameter/Range	Remarks
4	Criss-Cross Pattern Reproduced with Permission from [44], Elsevier, 2018		
		The Nusselt number in duct varies from 2.7 and 3.1 for inline and staggered.	Thermal-hydraulic performance varies between 1.2 and 1.5.
5	Circular and V-Type Turbulators Reproduced with Permission from [45], Elsevier, 2016		
		The various parameters with different values are taken for analysis.	Maximum enhancement attained when Nu no is 5.85 and f is 4.96.

### 3. Conclusions

The aim of this study was to review various shapes of artificial roughness geometry implemented in solar air heaters. A comparison of numerical and experimental analyses of different shapes of ribs with various parameters shows that artificial roughness results in enhanced heat transfer.

The salient information is.

1. Artificial roughness in solar air heaters results from better heat transfer and a reduced friction factor effect in SAH.
2. It is observed that the modified geometry of multiple V-shaped ribs with an inclined attack angle of  $60^\circ$  gives maximum thermal enhancement compared to the smooth duct.
3. It is found that a hyperbolic shape causes a reduction in the friction factor and enhanced heat transfer.
4. In contrast with other shapes, trapezoidal-shaped ribs in the flow direction will result in more turbulence for heat transfer inductance.
5. Discrete V-Down ribs suggest increasing the efficiency of pumping power to solar air heaters.
6. Investigational studies show that a Discrete Multiple V shape with a staggered rib is compared with a broken arc, S shape, L shape, W shape, Arc shape, and Circular with V shape, which gives the best overall thermal performances.

**Author Contributions:** V.K.B. and P.R.K. Conceived to collect various shape of ribs literature. G.M., J.T. and D.T. designed review study; V.K.B. wrote the paper; P.R.K. and H.T.T. analyzed the data and improved the draft and M.N.-O. assisted to draw figure. K.M. analyzed the role of angle of ribs.

**Funding:** This research received no external funding.

**Conflicts of Interest:** The authors declare no conflict of interest.

## Nomenclature

D	Hydraulic diameter of duct, m
e	Rib height, m
e/D	Relative roughness height
P	Pitch of the rib, m
P/e	Relative roughness pitch
G	Gap width, m
g/e	Relative gap width
Gd	Gap distance, m
Gd/Lv	Relative gap distance
H	Depth of duct, m
Lv	Length of single V-shaped rib, m
W	Width of duct, m
w	Width of single v-shaped rib, m
W/w	Relative roughness width ratio
Nu	Nusselt number of roughened duct
Nus	Nusselt number of smooth duct
fs	Friction factor of smooth duct
f	Friction factor of roughened duct
Re no	Reynolds number
f	Friction factor

## Greeks

A	Angle of attack, degree
H	Thermo-hydraulic performance parameter

## References

1. Luo, L.; Wen, F.; Wang, L.; Sundén, B.; Wang, S. Thermal enhancement by using grooves and ribs combined with delta-winglet vortex generator in a solar receiver heat exchanger. *Appl. Energy* **2016**, *183*, 1317–1332. [[CrossRef](#)]
2. Gupta, A.D.; Varshney, L. Performance prediction for solar air heater having rectangular sectioned tapered rib roughness using CFD. *Therm. Sci. Eng. Prog.* **2017**, *4*, 122–132. [[CrossRef](#)]
3. Al-Shamani, A.N.; Sopian, K.; Mohammed, H.A.; Mat, S.; Ruslan, M.H.; Abed, A.M. Enhancement heat transfer characteristics in the channel with Trapezoidal rib–groove using nanofluids. *Case Stud. Therm. Eng.* **2015**, *5*, 48–58. [[CrossRef](#)]
4. Moon, M.A.; Park, M.J.; Kim, K.Y. Evaluation of heat transfer performances of various rib shapes. *Int. J. Heat Mass Transf.* **2014**, *71*, 275–284. [[CrossRef](#)]
5. Gill, R.S.; Hans, V.S.; Saini, J.S.; Sukhmeet, S. Investigation on performance enhancement due to staggered piece in a broken arc rib roughened solar air heater duct. *Renew. Energy* **2016**, *104*, 148–162. [[CrossRef](#)]
6. Vipin, B.; Gawande, A.S.; Dhoble, D.B.; Zodpe, S.C. Experimental and CFD investigation of convection heat transfer in solar air heater with reverse L-shaped ribs. *Sol. Energy* **2016**, *131*, 275–295. [[CrossRef](#)]
7. Kumar, K.; Prajapati, D.R.; Samir, S. Heat Transfer and Friction Factor Correlations Development for Solar Air Heater duct Artificially Roughened with ‘S’ Shape Ribs. *Exp. Therm. Fluid Sci.* **2017**, *82*, 249–261. [[CrossRef](#)]
8. Lanjewar, A.; Bhagoria, J.L.; Sarviya, R.M. Heat transfer and friction in solar air heater duct with W-shaped rib roughness on absorber plate. *Energy* **2011**, *36*, 531–4541. [[CrossRef](#)]
9. Tanda, G. Performance of solar air heater ducts with different types of ribs on the absorber plate. *Energy* **2011**, *36*, 6651–6660. [[CrossRef](#)]
10. Eiamsa-Ard, S.; Promvong, P. Thermal characteristics of turbulent rib-grooved channel flows. *Int. Commun. Heat Mass Transf.* **2009**, *36*, 705–711. [[CrossRef](#)]
11. Bhushan, B.; Singh, R. Nusselt number and friction factor correlations for solar air heater duct having artificially roughened absorber plate. *Sol. Energy* **2011**, *85*, 1109–1118. [[CrossRef](#)]
12. Chandra, P.R.; Alexander, C.R.; Han, J.C. Heat transfer and friction behaviors in rectangular channels with varying number of ribbed walls. *Int. J. Heat Mass Transf.* **2003**, *46*, 481–495. [[CrossRef](#)]

13. Thakur, D.S.; Khan, M.K.; Pathak, M. Performance Evaluation of Solar Air Heater with Novel Hyperbolic Rib Geometry. *Renew. Energy* **2016**, *105*, 786–797. [[CrossRef](#)]
14. Yadav, A.S.; Bhagoria, J.L. A numerical investigation of square sectioned transverse rib roughened solar air heater. *Int. J. Therm. Sci.* **2014**, *79*, 111–131. [[CrossRef](#)]
15. Anil, K.; Man-Hoe, K. Effect of roughness width ratios in discrete multi V-rib with staggered rib roughness on overall thermal performance of solar air channel. *Sol. Energy* **2015**, *119*, 399–414. [[CrossRef](#)]
16. Kamali, R.; Binesh, A.R. The importance of rib shape effects on the local heat transfer and flow friction characteristics of square ducts with ribbed internal surfaces. *Int. Commun. Heat Mass Transf.* **2008**, *35*, 1032–1040. [[CrossRef](#)]
17. Pitak, P.; Petpices, E.A.; Withada, J.; Smith, E.A. Turbulent heat transfer and pressure loss in a square channel with discrete broken V-rib turbulators. *J. Hydrodyn.* **2016**, *28*, 275–283. [[CrossRef](#)]
18. Wang, H.T.; Lee, W.B.; Chan, J.; To, S. Numerical and Experimental Analysis of Heat Transfer in Turbulent Flow Channels with Two-Dimensional Ribs. *Appl. Therm. Eng.* **2015**, *75*, 623–634. [[CrossRef](#)]
19. Rajendra, K.; Solanki, S.C.; Saini, J.S. Thermo-hydraulic performance of solar air heaters having integral chamfered rib roughness on absorber plates. *Energy* **2001**, *26*, 161–176. [[CrossRef](#)]
20. Aharwal, K.R.; Gandhi, B.K.; Saini, J.S. An experimental investigation of heat transfer and fluid flow in a rectangular duct with inclined discrete ribs. *Int. J. Energy Environ.* **2009**, *1*, 987–998.
21. Skullong, S.; Kwankaomeng, S.; Thianpong, C.; Promvonge, P. Thermal performance of turbulent flow in a solar air heater channel with rib-groove turbulators. *Int. Commun. Heat Mass Transf.* **2014**, *50*, 34–43. [[CrossRef](#)]
22. Skullong, S.; Promvonge, P.; Thianpong, C.; Pimsarn, M. Heat transfer and turbulent flow friction in a round tube with staggered-winglet perforated-tapes. *Int. J. Heat Mass Transf.* **2016**, *95*, 230–242. [[CrossRef](#)]
23. Skullong, S.; Promvonge, P.; Thianpong, C.; Jayranaiwachira, N.; Pimsarn, M. Heat transfer augmentation in a solar air heater channel with combined winglets and wavy grooves on absorber plate. *Appl. Therm. Eng.* **2017**, *122*, 268–284. [[CrossRef](#)]
24. Hamid, M.O.; Zhang, B. Field synergy analysis for turbulent heat transfer on ribs roughened solar air heater. *Renew. Energy* **2015**, *83*, 1007–1019. [[CrossRef](#)]
25. Sharma, S.K.; Kalamkar, V.R. Experimental and numerical investigation of forced convective heat transfer in solar air heater with thin ribs. *Sol. Energy* **2017**, *147*, 277–291. [[CrossRef](#)]
26. Bagabir, A.M.; Khamaj, J.A.; Hassan, A.S. Numerical Study of Turbulent Periodic Flow and Heat Transfer in a Square Channel with Different Ribs. *J. Appl. Math. Phys.* **2013**, *1*, 65–73. [[CrossRef](#)]
27. Singh, S.; Chander, S.; Saini, J.S. Exergy based analysis of solar air heater having discrete V-down rib roughness on absorber plate. *Energy* **2012**, *37*, 749–758. [[CrossRef](#)]
28. Pankaj, P.; Harbindra, S. CFD Investigation on Heat Transfer Enhancement in Solar Duct with Slit Rib Roughness. *Res. J.* **2016**, *2*, 37–40.
29. AlokChaube, P.K.; Sahoo, S.C.S. Analysis of heat transfer augmentation and flow characteristics due to rib roughness over absorber plate of a solar air heater. *Renew. Energy* **2006**, *31*, 317–331. [[CrossRef](#)]
30. Kumar, R.; Goel, V.; Kumar, A. Investigation of heat transfer augmentation and friction factor in triangular duct solar air heater due to forward facing chamfered rectangular ribs: A CFD based analysis. *Renew. Energy* **2018**, 824–835. [[CrossRef](#)]
31. Saini, R.P.; Saini, S.K. Development of correlations for Nusselt number and friction factor for solar air heater with roughened duct having arc-shaped wire as artificial roughness. *Sol. Energy* **2008**, *82*, 1118–1130. [[CrossRef](#)]
32. Varun, R.P.; Saini, S.K. Investigation of thermal performance of solar air heater having roughness elements as a combination of inclined and transverse ribs on the absorber plate. *Renew. Energy* **2008**, *33*, 1398–1405. [[CrossRef](#)]
33. Varun; Patnaik, A.; Saini, R.P.; Singal, S.K. Performance prediction of solar air heater having roughened duct provided with transverse and inclined ribs as artificial roughness. *Renew. Energy* **2009**, *34*, 2914–2922. [[CrossRef](#)]
34. Anil, K. Analysis of heat transfer and fluid flow in different shaped roughness elements on the absorber plate solar air heater duct. *Energy Procedia* **2014**, *57*, 2102–2111. [[CrossRef](#)]
35. Jin, D.; Zhang, M.; Wang, P.; Xu, S. Numerical investigation of heat transfer and fluid flow in a solar air heater duct with multi V-shaped ribs on the absorber plate. *Energy* **2015**, *89*, 178–190. [[CrossRef](#)]

36. Singh, S.; Singh, B.; Hans, V.S.; Gill, R.S. CFD (computational fluid dynamics) investigation on Nusselt number and friction factor of solar air heater duct roughened with non-uniform cross-section transverse rib. *Energy* **2015**, *84*, 509–517. [[CrossRef](#)]
37. Yadav, A.S.; Bhagoria, J.L. A CFD (computational fluid dynamics) based heat transfer and fluid flow analysis of a solar air heater provided with circular transverse wire rib roughness on the absorber plat. *Energy* **2013**, *55*, 1127–1142. [[CrossRef](#)]
38. Alam, T.; Kim, M.H. Heat transfer enhancement in solar air heater duct with conical protrusion roughness ribs. *Appl. Therm. Eng.* **2017**, *126*, 458–469. [[CrossRef](#)]
39. Wang, Y.; Zhou, B.; Liu, Z.; Tu, Z.; Liu, W. Numerical study and performance analyses of the mini-channel with discrete double-inclined ribs. *Int. J. Heat Mass Transf.* **2014**, *78*, 498–505. [[CrossRef](#)]
40. Xie, G.; Zheng, S.; Zhang, W.; Sundén, B. A numerical study of flow structure and heat transfer in a square channel with ribs combined downstream half-size or same-size ribs. *Appl. Therm. Eng.* **2013**, *61*, 289–300. [[CrossRef](#)]
41. Singh, S.; Chander, S.; Saini, J.S. Investigations on thermo-hydraulic performance due to flow-attack-angle in V-down rib with gap in a rectangular duct of solar air heater. *Appl. Energy* **2012**, *97*, 907–912. [[CrossRef](#)]
42. Ravi, R.K.; Saini, R.P. Experimental investigation on performance of a double pass artificial roughened solar air heater duct having roughness elements of the combination of discrete multi V-shaped and staggered ribs. *Energy* **2016**, *116*, 507–516. [[CrossRef](#)]
43. Rajaseenivasan, T.; Srinivasan, S.; Srithar, K. Comprehensive study on solar air heater with circular and V-type turbulators attached on absorber plate. *Energy* **2015**, *88*, 863–873. [[CrossRef](#)]
44. Singh, P.; Ji, Y.; Ekkad, S.V. Experimental and numerical investigation of heat and fluid flow in a square duct featuring criss-cross rib patterns. *Appl. Therm. Eng.* **2018**, *128*, 415–425. [[CrossRef](#)]
45. Pandey, N.K.; Bajpai, V.K. Experimental investigation of heat transfer augmentation using multiple arcs with gap on absorber plate of solar air heater. *Sol. Energy* **2016**, *134*, 314–326. [[CrossRef](#)]



© 2018 by the authors. Licensee MDPI, Basel, Switzerland. This article is an open access article distributed under the terms and conditions of the Creative Commons Attribution (CC BY) license (<http://creativecommons.org/licenses/by/4.0/>).